# Implantable RF Medical Devices: The Benefits of High-Speed Communication and Much Greater Communication Distances in Biomedical Applications

**Article** *in* IEEE Microwave Magazine · June 2013

DOI: 10.1109/MMM.2013.2248586

CITATIONS
84

READS
2,069

**3 authors**, including:

Eric Chow
Cyberonics, Inc.
**20** PUBLICATIONS **789** CITATIONS

SEE PROFILE

Pedro P. Irazoqui
Johns Hopkins University
**133** PUBLICATIONS **3,607** CITATIONS

SEE PROFILE

FOCUSED ISSUE FEATURE

# Implantable RF Medical Devices

*Eric Y. Chow, Milton M. Morris, and Pedro P. Irazoqui*

In the early ages of implantable devices, radio frequency (RF) technologies were not commonplace due to the challenges stemming from the inherent nature of biological tissue boundaries. As technology improved and our understanding matured, the benefit of RF in biomedical applications surpassed the implementation challenges and is thus becoming more widespread. The fundamental challenge is due to the significant electromagnetic (EM) effects of the body at high frequencies. The EM absorption and impedance boundaries of biological tissue result in significant reduction of power and signal integrity for transcutaneous propagation of RF fields. Furthermore, the dielectric properties of the body tissue surrounding the implant must be accounted for in the design of its RF components, such as antennas and inductors, and the tissue is often heterogeneous and the properties are highly variable. Additional challenges for implantable applications include the need for miniaturization, power minimization, and often accounting for a conductive casing due to biocompatibility and hermeticity requirements [1]–[3]. Today, wireless technologies are essentially a must have in most electrical implants due to the need to communicate with the device and even transfer usable energy to the implant [4], [5]. Low-frequency wireless technologies face fewer challenges in this implantable setting than its higher frequency, or RF, counterpart, but are limited to much lower communication speeds and typically have a very limited operating distance. The benefits of high-speed communication and much greater communication distances in biomedical applications have spawned numerous wireless standards committees, and the U.S. Federal Communications Commission (FCC) has allocated numerous frequency bands for medical telemetry as well as those to specifically target implantable applications. The development of analytical models, advanced EM simulation software, and representative

*Eric Y. Chow (eric.chow@cyberonics.com) and Milton M. Morris (milton.morris@cyberonics.com) are with Cyberonics, Inc., Houston, Texas. Pedro P. Irazoqui (pip@purdue.edu) is with Purdue University, West Lafayette, Indiana.*

*Digital Object Identifier 10.1109/MMM.2013.2248586*
*Date of publication: 7 May 2013*

 1527-3342/13/$31.00©2013IEEE 


© IMAGESOURCE

RF human phantom recipes has significantly facilitated design and optimization of RF components for implantable applications.

## Frequency Bands for Medical RF Communication and MedRadio

In the past couple decades, the FCC has been increasing its focus on medical communications and dedicating numerous new bands in the frequency spectrum to these associated applications. Back in 1947, the FCC established the industrial, scientific, and medical (ISM) bands, which they did not initially intend for communication [6]. The ISM bands are unlicensed and, as a result, the bands are relatively noisy and users have little-to-no regulatory protection. More recent advances in RF technology, including new modulation types, multiplexing schemes, and other novel methods, have now enabled a multitude of devices to successfully and reliably communicate in these bands. Medical devices most commonly use the 433 MHz, 900 MHz, 2.45 GHz, and 5.8 GHz ISM bands, where the FCC emissions regulations and power-level requirements are more relaxed; however, specific absorption rate (SAR) considerations are still required [58]. About 40 years ago, the FCC allowed biomedical telemetry applications to utilize the 460–470 MHz band, part of the private land mobile radio service (PLMRS) band, but only as a secondary user, meaning that those medical applications must tolerate interference from the PLMRS primary users but not itself cause any interference. Medical telemetry devices used to also utilize the previously unused portions of the television bands (174–216 MHz) and (470–668 MHz); however, the emergence of digital television is now targeting usage of these bands.

On 12 June 2000, the FCC specifically allocated the 608–614 MHz, 1,395–1,400 MHz, and 1,429–1,432 MHz bands for wireless medical telemetry service (WMTS) applications, typically devices worn on the patient's body, and used for untethered monitoring of patient health parameters [7]. Just recently, in 2012, the FCC allocated the 2,360–2,400 MHz band for multiple body area network (MBAN) applications, networking of multiple body transmitters used for performing measurements, diagnostics, or therapeutic functions [8]. Medical devices have also begun exploring the 3.1–10.6 GHz ultrawideband (UWB) spectrum, which the FCC approved on 14 February 2002 for a broad range of applications [9]–[11].

The FCC has also been allocating spectrum specifically for just implantable medical device applications, and it established the 402–405 Medical Implant

Communications Service (MICS) band on 19 November 1999 [12], [13]. Shortly after the FCC established the MICS band, major players in the medical device industry began releasing MICS-based devices, including Biotronik in 2003, Medtronic in 2004, and St. Jude in 2006 [14]–[16]. On 20 March 2009, the FCC renamed this band the Medical Device Radio Communication Service (MedRadio) and extended the spectrum to 401–406 MHz [17], [18]. On 30 November 2011, the FCC added four additional bands (413–419, 426–432, 438–444, and 451–457 MHz) to the MedRadio spectrum, specifically targeting neuromuscular microstimulation implantable applications in medical micropower networks (MMNs) [19] [20]. As mentioned above, the FCC allocated the 2,360–2,400 MHz, which is considered part of MedRadio but does not specifically target implantable applications. The 401–406 MHz band is the spectrum of most interest to the general implantable device industry, and the FCC has set strict rules on this band to ensure interoperability. In [21], the rules are described in detail and restrictions on usage modalities (listen-before-talk), power levels ($< 25\ \mu W$),and bandwidth (100, 150, and 300 kHz) are included. The 401–406 MHz frequency range provides a band with low interference and decent bandwidth as well as a reasonable balance between body effects such as attenuation and relatively efficient antenna designs. The most widely used commercially available MICS transceiver chip set is available through Zarlink Semiconductor [22]. The Zarlink transceiver accurately follows the MICS standard, communicates at rates of 200–800 kb/s, and consumes around 5 mA. Recent work in RFIC design has developed very-low-power transmitters and transceivers that operate at the MICS frequency band. Work presented in [23] and [24] show data rates around 100–250 kb/s with around 300–500 $\mu$W of power, and [25] achieves 200 kb/s with a power consumption of only 90 $\mu W$.

## Analytical Modeling of the Biological Implanted Environment and RF Design

The human body is a heterogeneous media consisting of multiple layers of tissue with varying dielectric properties. A representative model for RF design should account for these layers and for reasonable analytical calculations, these layers can be simplified to rectangular slabs. More detailed contours and textures can be incorporated into EM simulation software, such as ANSYS High-Frequency Structural Stimulator (HFSS) or Computer Simulation Technology (CST) Microwave Studio (MWS), where the structures are broken down into a tetrahedral-based mesh network. For implantable RF antenna design, the major considerations are

- tissue absorption
- interfaces between layers and corresponding reflections
- antenna matching in the implanted environment.

The tissue absorption is the amount of EM energy that is reduced after passing through a homogeneous media. Since the human body is quite heterogeneous, different absorptive properties need to be considered as the RF signal passes through the various media. The effect on signal power due to absorption in a particular material is an exponential decay as a function of distance and a factor known as the attenuation coefficient [26]. This attenuation coefficient represents how difficult it is for energy to travel through the particular media and is a function of the media's dielectric properties and the frequency of interest. A method to calculate the overall effect of just tissue absorption on a particular propagation is to take a superposition of the results from evaluating the signal loss independently in each material. Since the relationship is exponential with distance, all but just-underneath-the-skin implants will see an effect with the significance growing rapidly with implantation depth.

The heterogeneous nature of the human body presents a multitude of interfaces between varying materials where the boundary conditions of the interfaces themselves can have a significant effect on the signal propagation. The magnitude of the effect depends on the geometries and thicknesses of the layers and their corresponding dielectric properties. When an EM signal is traveling from one tissue-type to another, the impedance difference between the two tissue-types results in a reflection of some energy, which reduces the power of the signal that travels to the other side of the interface. The boundary condition relationships derived from Maxwell's equations describe the effect of each interface on the signal [27]. The effect of these reflections, relative to that from just tissue absorption, is more significant for a relatively higher density of layers in the signal path where the dielectric properties of the neighboring layers are drastically varied. Implantable medical devices, such as pacemakers, are often placed somewhere between a depth of about 1 in and the surface of the skin where the primary interfaces are between muscle, fat, skin, and air. If the implant is placed deep in the muscle in a patient with very thin fat and skin layers, then the absorption effect will dominate. Conversely, if the implantation is shallow and goes through equally thick layers of muscle, followed by fat, followed by skin, then the effect of the interface reflections may dominate.

The tissue surrounding the antenna of an RF implanted medical device has a significant effect on the impedance and resonance frequency of the antenna and will detune the antenna from its free-space performance [28], [29]. The effect of the implanted environment is dependent on the dielectric properties of the surrounding media. For an analytical model, a useful simplification of the surrounding environment is using a single dielectric with properties derived from a weighted average of the permittivity and conductivity of the nearby tissue types, with the weighting positively correlated with the corresponding tissues' proximity to the antenna.

In the mid-1990s, Camelia Gabriel, Sami Gabriel, and their team developed an extremely useful database of the dielectric properties of body tissues at RF and microwave frequencies [30]–[32]. This database presents data that shows, for RF frequencies, that dielectric properties of skin and muscle are not too dissimilar. At 400 MHz, skin and muscle have relative permittivities of 47 and 57 and conductivities of 0.7 and 0.8 S/m, respectively. The relative permittivity and conductivity of fat, however, are quite a bit different with values of about 5.6 and 0.04 S/m respectively. From a tissue absorption perspective, due to the higher permittivity and conductivity values, the skin and muscle will have a more significant effect on the signal than fat for a given thickness. Often, however, a medical implant is just below the fat and on the surface of the muscle, but not beneath any muscle, as is typically the case for pacemakers and implantable cardiac defibrillators, and if the skin layer is much thinner than the fat section that the signal propagates through, the fat section in these cases may actually be the material that absorbs the most EM energy. For medical implants, RF communication typically traverses layers of alternating high and low dielectric property values from muscle, through fat, through skin, and then into the air. The large variance between neighboring layers results in significant reflections, which reduce the strength of the signal that traverses through the layers. If the implanted antenna is inside the fat layer and the thickness of the skin is very small with respect to the wavelength, which is a common case for medical devices, then the effect of reflections is reduced because the thinness of the skin results in transparency and the dielectric properties of fat are not too different than that of air. The similarity of the dielectric properties of fat with that of air reduce the detuning and impedance change that the fat would have on the antenna with respect to its performance in air; however, the high dielectric muscle and skin are typically nearby, which will significantly affect the antenna properties.

Accounting for tissue absorption, reflections due to interface layers and antenna detuning, and impedance changes, and utilizing the dielectric property data of human body tissues to derive an analytical model provides a useful initial step to implanted antenna design. Although the analytical calculations encompass significant simplifications to the surrounding geometries as well as utilization of the far-field plane-wave approximation, the derived relationships are still necessary to provide initial design guidance and help with the understanding of the EM effects of the implanted environment.

## EM Simulation Software, Modeling, and Design Optimization

There are numerous advanced EM simulation tools for considerably advancing the model after the initial design and guidance from the analytical assessment. Full-wave three-dimensional (3-D) EM software provides the capability for implementing a relatively comprehensive model of the antenna and the human body. Full-wave simulation tools consider all the time-varying components in Maxwell's equations and do not make assumptions about field relationships, whereas other solver-types (i.e., quasistatic) solve for only certain modes, typically just transverse EM, and approximates the time-derivatives typically defining them as zero. Additionally, an important aspect for biomedical implantable applications is that full-wave solvers accurately capture losses due to radiation.

Among modern-day full-wave simulators, there are three main types: method of moments (MoM), finite element method (FEM), and finite-difference time-domain (FDTD). For human-body modeling, MoM is not ideal because it uses a surface mesh and thus cannot accurately model complex dielectric structures such as the tissue geometries and interfaces. FEM and FDTD achieve greater accuracy for this application because they utilize volume meshing. FEM solves in the frequency domain and can often more accurately handle complicated geometries, such as curved objects and the heterogeneous human body, due to its use of tetrahedral meshing with variable element sizes [33]. FDTD solves in the time-domain, making it good for capturing large frequency ranges, and its simplicity can often lead to more efficient simulations, but it is limited to more rectangular shapes that may increase the difficulty and/or accuracy in human-body modeling [34].

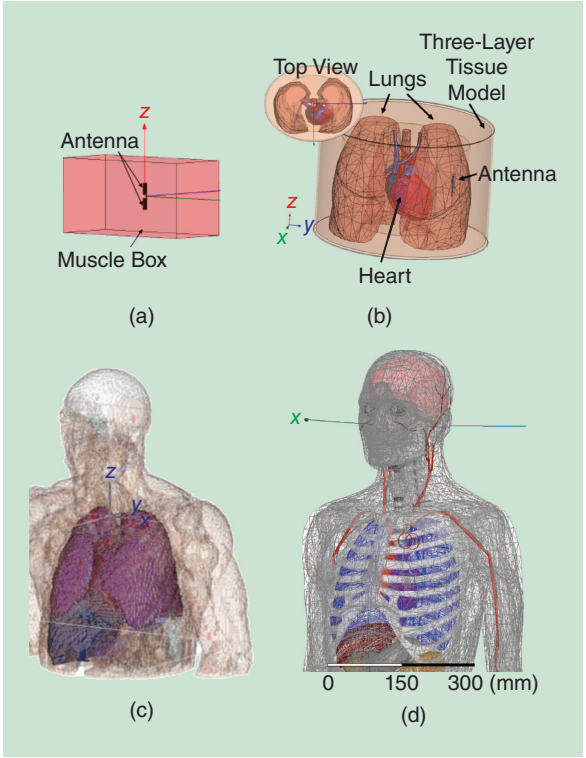


**Figure 1.** *(a) The simplified model, (b) the intermediate model, (c) the CST HUGO model, and (d) the ANSYS human-body model [40], [41].*

A popular full-wave 3-D simulator that employs FEM is ANSYS HFSS, and one that utilizes FDTD is CST MWS. An additional advantage of both of these tools is that they already have human-body models available. CST's human-body model, called HUGO, is a model of slices consisting of several thousand layers, 32 tissue types, and down to a 1 mm resolution. ANSYS's human-body model consists of 300+ objects (bones, muscles, organs), about 1/2 million tetrahedral, and also has accuracies down to the millimeter level. Modern-day advanced EM software have demonstrated that computational techniques and existing human-body models are accurate enough such that the FCC deems the FDTD method and FEM are sufficient for showing compliance with RF exposure limits, per 47 CFR §95.1221 and DA 11-192 respectively [35]–[37].

Utilizing different levels of simulation fidelity through the simulation design phases optimizes the design-time efficiency. Beginning with a simple model such as a box with the appropriate dielectric properties, as shown in Figure 1(a) or one described in [38], or a simple structure with just a few layers allows for coarse design and antenna tuning. An intermediate model encompassing some of the larger structures, i.e., nearby organs as shown in Figure 1(b), improves the accuracy, allowing for finer design optimization while maintaining reasonable simulation times. A final comprehensive model provides the highest level of accuracy in the simulation environment, but its lengthy simulation time requirement limits this to the end of the simulation environment design phase where the antenna is already close to its final implementation. The CST Studio HUGO and ANSYS HFSS human-body models are shown in Figure 1(c) and (d), respectively. Additional simulation permutations incorporating different body types and positions, as described in [39], are useful in more closely mimicking the precise implantation environment and use-case.


(a)

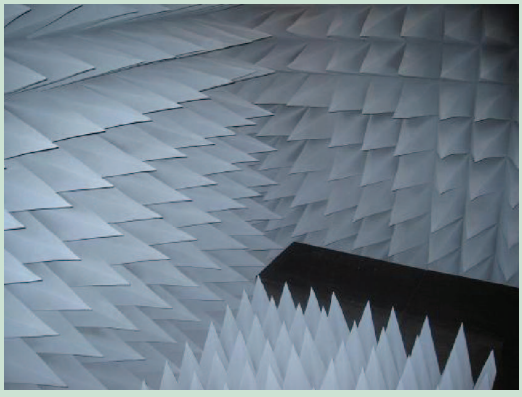
(b)

**Figure 2.** *An anechoic chamber (a) shield and (b) RF absorbent foam.*

## Physical Testing and RF Phantoms

A representative lab testing environment allows for efficient and comprehensive testing of the physical antenna or multiple antennas developed in the simulation design phase. An RF anechoic chamber is crucial for obtaining consistent and repeatable results. A typical chamber is composed of two main parts, a conductive exterior and an RF absorbent interior. The conductive exterior, shown in Figure 2(a), acts as a Faraday cage and shields the testing environment from outside noise, typically offering well over 100 dB of isolation at RF frequencies. The interior of the chamber is covered with an RF absorbent material, shown in Figure 2(b), which significantly reduces the multipath that would otherwise lead to variations from constructive/destructive interference, frequency distortion, and time/phase delay spreading. Essentially, an ideal anechoic chamber mimics an infinitely sized open space with no external radiation noise and no walls or other obstacles present, thus allowing for direct line-of-sight measurements and clean evaluation of the isolated effects of just the device under test.

The two most commonly used radiation-absorbent materials are carbon-iron-based foam, fabricated in pyramidal cones to minimize reflectivity, and ferrite-based tiles. Utilizing a high-performance pyramidal absorber available from Cuming Microwave, achieving a reasonable reflectivity of −30 dB for operation down to 300 MHz requires a cone length of 2 ft (610 mm) [42]. Typically, cones are oriented such that they point normal to an incoming RF plane wave such that the foam presents a tapered impedance, gradually absorbing the energy as the signal progresses through the length of the cone, but techniques are sometimes used with strategically positioned smaller wedge-shaped foam, which divert the energy to a wall where the longer pyramidal cones are present. The alternative material, ferrite-based tile, has a complex relative permeability, which is dependent on frequency, and for a frequency range of about 160–180 MHz is close to its relative permittivity, resulting in low reflectivity due to a wave impedance near that of

free space (377 Ω). Typically, near the optimal frequency, the reflectance can be less than −40 dB but outside of 30 MHz to about 500 MHz, the reflectance will rise above −20 dB. Ferrite tile is relatively expensive but can reduce the chamber size requirements, especially for the lower frequency ranges, and actually result in lower overall cost. A third option is a higher-cost hybrid combination of ferrite-tile and foam, which may offer a wider range of operation, encompassing the lower frequency ranges.

When designing the chamber dimensions, the designer must keep in mind that the maximal absorptivity of the interior chamber walls occurs at normal incidence. Design considerations should sufficiently satisfy the far-field approximation for the signals emanating from the device(s) under test and incident on the interior wall. In some cases, if size and cost factors are acceptable, a circular room may offer the most optimal solution as it can present a normal incidence boundary for the entire azimuthal plane around the point source.

An implanted setting is required to produce relevant results and the use of a representative human-body phantom, prior to ex vivo and in vivo trials, allows for comprehensive testing and consistent repeatable results. Shortly after the MICS band was established in 1999, the FCC updated their rules and regulations [see CFR47 §95.639(f)(2)(i)], to include guidance on measurement appropriating a human-torso simulator consisting of a cylindrical Plexiglas container [43]. In 2009, the FCC removed that section to provide greater testing flexibility and expand compliance options as described in [44] but keeps the guidance available in [45]. In [35], the OET Bulletin 65 Supplement C (Ed. 01–01), an appropriate RF human phantom tissue recipe is presented for a variety of frequencies utilizing mixtures of water, salt, sugar, hydroxyethyl cellulose (HEC), bactericide, Triton X-100, and diethylene glycol butyl ether (DGBE). This RF phantom recipe and its specific materials are based primarily on the work presented in [46]. Solid materials such as Play-Doh or similar modeling compounds and rubber are sometimes used to mimic additional layers such as fat. The target application may require variations of phantom form-factor as well as differing tissue recipes. For example, a rectangular

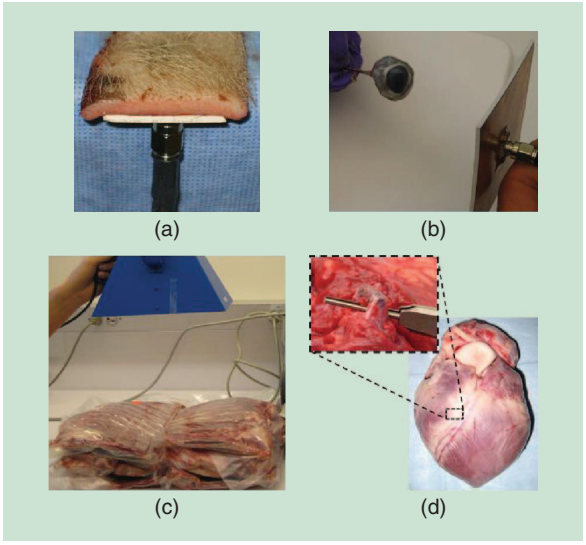


**Figure 3.** *Ex vivo studies [47], [48].*

form-factor incorporating a fat mimicking phantom layer may be more appropriate for some torso-based implant applications. A spherical-type structure may be more appropriate for head modeling applications. A fully accurate human body form-factor is typically not necessary for the accuracy that is expected at this stage, although, depending on the use case, mimicking of the limbs may provide some more insight specific to the use-case. Rotation platforms, preferably plastic or made out of another RF-transparent material, and support for different body position testing allows for measurement of a more comprehensive antenna radiation pattern.

## Ex Vivo and In Vivo Studies

Measurements and studies done on real biological tissue is the final stage of design verification and validation. Testing using deceased tissue or cadavers (ex vivo), prior to engaging in full-fledged live animal and clinical trials (in vivo), provides a useful testing model, and the corresponding measurement data is useful for additional design adjustments. Performing these initial ex vivo studies is a good risk-reduction step and helps with surgical set-up prior to entering the more involved and higher cost

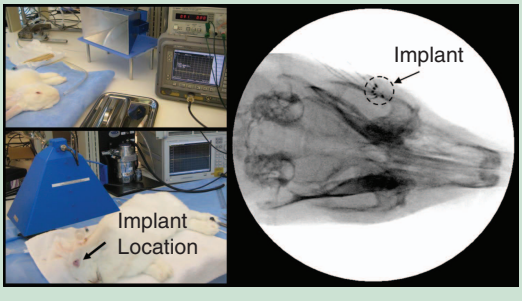


**Figure 4.** *In vivo ocular implant studies [50].*

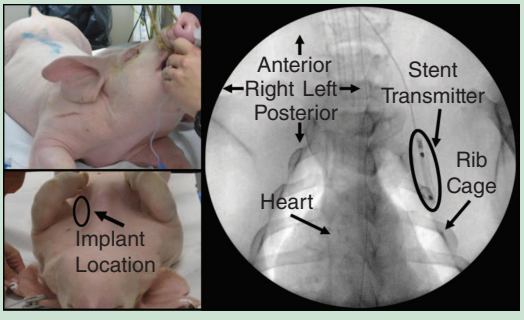


**Figure 5.** *In vivo cardiovascular studies [41].*

live animal and clinical trials (in vivo). A quick simple measurement done with a network analyzer is shown in Figure 3(a), where the performance of received power is evaluated with and without a piece of excised tissue placed over a patch antenna, and the results showed about a 15 dB power reduction due to the tissue [47]. Note that the set-up is acceptable for relatively large antennas and patch-type antennas, which have a ground plane to prevent stray fields from coupling onto the large subminiature version A (SMA) ground shield, but for miniature antennas, accurate measurements require elimination of the cable or use of ferrite beads. For an ocular implant application, the cable is eliminated in [48] through the use of an implantable transmitter IC and a miniature antenna and, as shown in Figure 3(b), ex vivo measurements are performed in an excised porcine eye utilizing a patch antenna and a spectrum analyzer. Measurements showed a power reduction of up to 6 dB, due to boundary reflections and attenuation, when implanted 1.5 mm beneath the surface of the eye, behind the cornea and scleral tissue. Studies shown in Figure 3(c) incorporate more of the surrounding tissue, mainly the ribs and torso area, and the

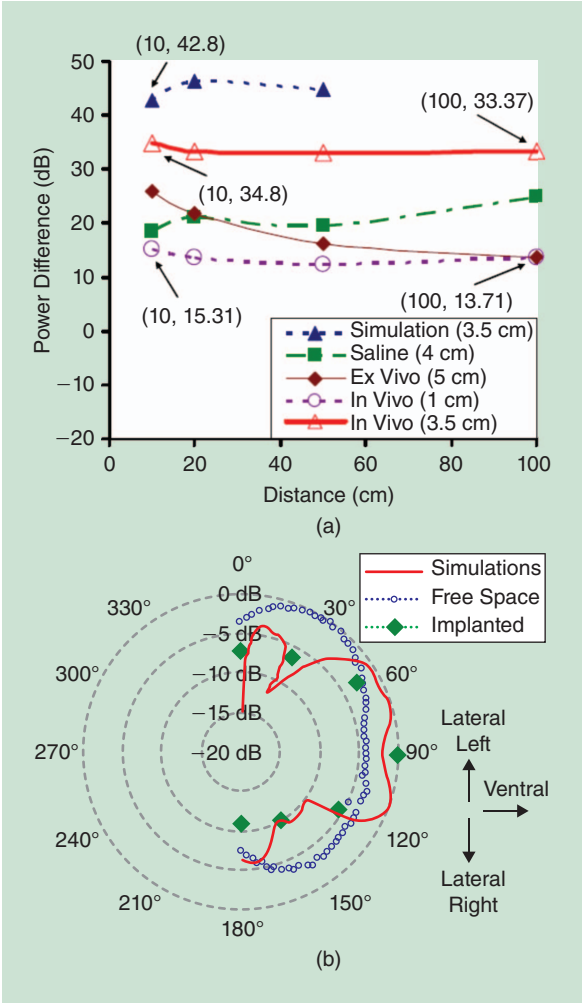


**Figure 6.** *In vivo porcine (a) antenna transmission and (b) pattern plot compared with simulated results [40], [41].*

experiment shown in Figure 3(d) included the heart and involved an implantation in a vessel near the organ, both utilizing an implantable transmitter and antenna, with measurements taken through a wideband horn antenna and spectrum analyzer.

The ex vivo testing phase vets out some more risk, helps with the surgical set-up, provides a close representation of what to expect from the antenna in a clinical setting, and allows for some additional tuning prior to entering the in vivo studies. The in vivo testing is the most accurate method to quantify the effects of surrounding biological tissue on RF propagation. Compared to the ex vivo studies, the set-up for in vivo experiments is substantially more involved. Organizations such as the Institutional Animal Care and Use Committee (IACUC), has comprehensive and stringent rules for any type of testing on live animals. It is required for any animal testing facility to submit a detailed protocol for the surgical procedure and testing that is intended. The protocol for an acute in vivo test must have all presurgical animal preparation, surgical details, and testing set-up details through the termination of the test subject, where the time between anesthetic induction and euthanization is on the order of hours. For a chronic (on going) study, the protocol is quite a bit more involved, as the surgical procedural rules are more stringent and it must include details of the longer-term care for the animal and testing throughout the chronic study. The protocol must ensure that the study follows all the rules set by the IACUC, and the approval process is usually lengthy as the committee thoroughly reviews the protocol. Often, the committee requests changes, and the protocol may go through several iterations of submission and review as the committee ensures all rules are closely followed. The animal study can only commence after protocol approval by the IACUC or another certified animal use and care committee.

Work done in [49] and [50] for ocular implant applications involved acute testing on live New Zealand white rabbit subjects, shown in Figure 4. This specific species of rabbit has relatively large eyes, and their size is similar to that of human eyes. Surgery and testing done in this work followed a Purdue Animal Care and Use Committee (PACUC) approved protocol (PACUC No. 08–004). The rabbits are first caged, maintained, and monitored for one week prior to surgery. On the day of the surgery, anesthetic induction is done using a ketamine-xylazine injection in the leg muscle and maintained with an intravenous Propofol drip through a vein in the ear and a proparacaine eye-drop applied every 10 min. For these RF propagation studies, a miniature device with a 2.4-GHz transmitter and antenna is implanted in the suprachoroidal space, about 1 mm beneath the surface of the eye. Measurements show that the power of the 2.4-GHz RF signal reduced by about 4–5 dB due to tissue absorption and boundary reflections.

Studies described in [40] involve acute in vivo testing on porcine test subjects, as shown in Figure 5, for cardio-thoracic applications. Again, due to the strict

regulations surrounding in vivo studies, the studies strictly followed a PACUC-approved protocol (PACUC No. 08–019). For this surgery, the subject is first anesthetized with a Telazol (250 mg tiletamine and 250 mg zolazepam), ketamine (250 xmg), and xylazine (250 mg) combination. Anesthesia maintenance is accomplished with an isoflurane (1.5–4.0% oxygen) inhalation anesthetic administered from a machine with a vaporizer and a waste gas ventilation system. The surgery involved implantation of a stent-based antenna, integrated with a miniature 2.4-GHz transmitter, at a depth of 3.5 cm. The results of these in vivo studies showed a power loss of 33–35 dB due to boundary reflections and tissue attenuation effects.

If further design optimization is desired, it is useful to first evaluate the accuracy of the simulation models by comparing the in vivo results with those done using the EM simulation software. Adjustments to increase the accuracy of the EM simulation model can help improve the next antenna design iteration. The simplest simulation model, the box with the dielectric properties of muscle, was accurate to within 10 dB when compared with the porcine in vivo measurements [40], [51]. The simulation model incorporating several components of ANSYS's human-body model was accurate to within 3–5 dB when compared with the in vivo porcine testing results [41]. The implanted location and surrounding structures will undoubtedly affect the antenna pattern, and the work in [41] shows a stent-based antenna with a near-omnidirectional pattern in free-space but an altered pattern in the implanted setting, shown in both the simulation environment and the in vivo measurements. Figure 6(a) shows the power reduction (power difference) due to tissue affects determined by the difference of a received power measurement done in free-space and that done in an implanted setting (simulation, phantom, ex vivo, and in vivo). Figure 6(b) shows a comparison of the radiation pattern between the simulation results and the data gathered from the in vivo studies, which took measurements at discrete points in the front hemisphere of the porcine test subject.

These models provide a useful tool for antenna and impedance matching network design iterations. To further improve and optimize the network to help account for the multitude of application specific variability, automated closed-loop matching technique provide a good option. Work presented in [52] describes a system that determines the actual input impedance of the antenna and tunes the matching network accordingly. Performing this automated matching in the final implanted setting results in a matching network that is truly optimized for the specific use case environment.

## Revolutionizing the Implantable Device Industry

The implantable electronic device industry saw its earliest mainstream success with the cardiac pacemaker. In 1958, Rune Elmqvist and Åke Senning developed an internal pacemaker and implanted the device into a patient, Arne H. W. Larsson, in Sweden, marking the first successful human pacemaker implant [53], [54]. The advent of the semiconductor transistor, just ten years prior, made the development of that pacemaker possible and is one of the key enabling technologies for the field of electronic implantable devices [55]. The once-large devices have evolved into very small pacemakers and cardioverter defibrillators that, aside from providing great therapeutic benefit, can now communicate important diagnostic information about a subject/patient and about itself (device status). The global cardiac rhythm management (CRM) industry, which includes pacemakers and defibrillators, is forecasted to reach US$22.3 billion by 2015, with implantable devices consisting of over half that market [56]. The explosion and globalization of implantable devices in cardiac applications has spawned their use in a multitude of other indications and driven rapid advancement of related electronic technologies.

The basic concepts of direct tissue stimulation used by the first implantable pacemakers have been broadened to include the nervous system (neuromodulation) and have inspired the development of implantable functional instrumentation that, among other things, are used for measuring and reporting pressure or transporting fluids (e.g., blood). Implantable neuromodulation systems have been advanced to address pathologies from gastroesophageal reflux disease (GERD), sleep apnea, chronic pain, Parkinson's, Alzheimer's, obesity, epilepsy, hypertension, heart failure, and compromises to auditory and vision function. Cochlear implants are discretely enabling the improvement of hearing. Mechanical hearts and left ventricular assist devices (LVADs) are designed to increase a human's forward flow of blood thereby extending and improving their lives. From the hypoglossal nerve to the vagus, from the phrenic nerve to the spinal cord, from the heart to the head, the ears and the eyes, there is a new frontier for implantable devices. Each has its own unique set of challenges and most have the unique opportunity to monitor, measure, diagnose, and report key diagnostics that can lead to better insights into a patient's well-being. In an emerging world of "Big Data" where protected health information, if available, can be served up at a caregiver's command, finding low-power, high-fidelity, and broad-bandwidth approaches to liberating key diagnostics brings great promise to patient care. However, in the electronic implantable device field where there is significant tissue-based RF effects and ultra-low power and miniature form factors are crucial, such communication solutions remain a challenge to develop.

Near-field inductive coupling technology introduced the option of wireless communication to implantable devices allowing remote connection to an external programming device (with an inductive wand). This communication link has traditionally been used for

programming the device and for retrieving important device centric information such as battery status. During the surgical implant procedure, the wand is brought into the sterile field and thus requires sterilization. During the follow up and technical servicing of an implant, the patient is typically required to place the wand directly over their device, which can be difficult if the device is difficult to find beneath the skin or the patient is not capable of remaining still during the communication process. The relatively slow data-rates result in an oftentimes lengthy data-transfer period and misalignment of the wand over the implant during the communication session may cause breaks in the inductive link.

The advent of far-field RF communication links in electronic implantable medical devices alleviates many of these issues and drives a higher perceived ease-of-use. This communication advancement eliminates the need for a wand in the sterile field and physicians can begin to suture up a patient while communicating with the device to verify its operation. Far-field RF technology relieves the necessity of patients assisting with holding a wand, precise alignment, and searching for the implant and appeases the issue of patient movement during the communication session. Devices could now use their wireless communication capabilities to transmit their functional status to a base station in the home. The base station could be used by the patient, family members, or caregivers to review device functional status and programming as well as certain patient diagnostics that are collected by the implanted device. This advanced patient management system helped to form new revenue opportunities for major companies in the industry (e.g., Carelink from Medtronic, Inc, and Latitude from Boston Scientific Corporation) but also gave physicians, patients, and family members an opportunity for improved managed care through better, more accessible data [15], [57]. Alas, these great advances have largely been isolated to the area of care that pioneered the genre, cardiac pacemakers and defibrillators.

## Conclusion

The rapidly accelerating growth of the medical device field has turned to RF as a key technology. The FCC has confirmed its importance through allocation of frequency bands specific to medical applications and RFIC chip sets developed by both research groups and industry have supported operation in these bands. Analytical modeling and simulations offer solutions for initializing an antenna and matching network design while subsequent empirical testing is necessary. An anechoic chamber provides a noise and multipath-free testing environment for consistent and repeatable results. An RF phantom and/or ex vivo tissue model the implanted environment and oftentimes allows for relatively simple and quick measurement set-ups. The final, most accurate test is that done in vivo. The cardiac pacemaker and defibrillator market has pervasively integrated RF into their devices, but we are just beginning to see RF technology permeate into other applications of implantable electronics such as neurostimulators and internal monitoring devices. There is still work to be done and the most exciting diagnostic information is still in front of us, untapped, waiting to be liberated, and in need of the emerging RF technology for implantable devices.

## References


[1] M. Yuce and T. Dissanayake, "Easy-to-swallow wireless telemetry," *IEEE Microwave Mag.*, vol. 13, no. 6, pp. 90–101, 2012.

[2] E. Y. Chow, D. Ha, T. Lin, W. N. de Vries, S. W. John, W. J. Chappell, and P. P. Irazoqui, "Sub-cubic millimeter intraocular pressure monitoring implant to enable genetic studies on pressure-induced neurodegeneration," in *Proc. Engineering Medicine Biology Conf.*, Buenos Aires, Argentina, 2010, pp. 6429–6432.

[3] E. Y. Chow, S. Chakraborty, W. J. Chappell, and P. P. Irazoqui, "Mixed-signal integrated circuits for self-contained sub-cubic millimeter biomedical implants," in *Proc. Int. Solid State Circuits Conf.*, San Francisco, CA, 2010, pp. 236–237.

[4] E. Y. Chow, A. Chlebowski, W. J. Chappell, and P. P. Irazoqui, "Fully wireless implantable cardiovascular pressure monitor integrated with a medical stent," *IEEE Trans. Biomed. Eng.*, vol. 57, no. 6, pp. 1487–1496, 2010.

[5] E. Y. Chow, A. L. Chlebowski, and P. P. Irazoqui, "Miniature implantable RF-wireless active glaucoma intraocular pressure monitor," *IEEE Trans. Biomed. Circuits Syst.*, vol. 4, no. 6, pp. 340–349, 2010.

[6] The International Telecommunication Union, "Documents of the international radio conference—Doc. no. 1–100," in *Proc. Int. Radio Conf.*, Atlantic City, NJ, 1947, pp. 18E–58E.

[7] Federal Communications Commission, "§ 95.630 WMTS transmitter frequencies," in "Code of Federal Regulations, Title 47—Telecommunication, Chapter 1—FCC, Subchapter D—Safety and Special Radio Services, Part 95—Personal Radio Services, Subpart E—Technical Regulations," Tech. Rep. 95.630, 2000.

[8] Federal Communications Commission, "§ 95.628 Medradio transmitters in the 413-419 MHz, 426-432 MHz, 438-444 MHz,and 451-457 MHz and 2360-2400 MHz bands," in "Code of Federal Regulations, Title 47—Telecommunication, Chapter 1—FCC, Subchapter D-Safety and Special Radio Services,Part 95—Personal Radio Services, Subpart E—Technical Regulations," Tech. Rep. 95.628, 2012.

[9] A. Ghildiyal, K. Amara, R. Molin, B. Godara, A. Amara, and R. Shevgaonkar, "UWB for in-body medical implants: A viable option," in *Proc. Ultra-Wideband, IEEE Int. Conf.*, Nanjing, China, 2010, pp. 1–4.

[10] J. Wang and D. Su, "Design of an ultra wideband system for in-body wireless communications," in *Proc. Environmental Electromagnetics, The 4th Asia-Pacific Conf.*, Dalian, China, 2006, pp. 565–568.

[11] Federal Communications Commission, "FCC 02-48, ET Docket 98-153," in "Revision of Part 15 of the Commission's Rules Regarding Ultra-Wideband Transmission Systems," Tech. Rep. 98-153, 2002.

[12] Federal Communications Commission, "WT Docket No. 99-66, RM-9157," in "Amendment of Parts 2 and 95 of the Commission's Rules to Establish a Medical Implant Communications Service in the 402-405 MHz Band," Tech. Rep. 99-66, 1999.

[13] Federal Communications Commission, "Subpart I—medical implant communications," in "Code of Federal Regulations, Title 47—Telecommunication, Chapter 1—FCC, Subchapter D-Safety and Special Radio Services, Part 95—Personal Radio Services," 1999.

[14] Biotronik SE and Co. KG. (2013). [Online]. Available: http://www.biotronik.com

[15] Medtronic, Inc. (2013). [Online]. Available: http://www.medtronic.com/

[16] St. Jude Medical, Inc. (2013). [Online]. Available: www.sjm.com

[17] Federal Communications Commission, "ET Docket No. 06-135," in "FCC Adopted Rules for New Advanced Medical Technologies," Tech. Rep. 06-123, 2009.

[18] Federal Communications Commission, "Subpart I—medical device radiocommunication service," in "Code of Federal Regulations, Title 47—Telecommunication, Chapter 1—FCC, Subchapter D—Safety and Special Radio Services, Part 95—Personal Radio Services," Tech. Rep., 2009.

[19] Federal Communications Commission, "FCC 11-176, ET Docket No. 09-36," in "Amendment of Parts 2 and 95 of the Commission's Rules to Provide Additional Spectrum for the Medical Device Radiocommunication Service in the 413-457 MHz Band," Tech. Rep. 09-36, Washington, D.C., 2011.

[20] Federal Communications Commission, "§ 95.628 MedRadio transmitters in the 413-419 MHz, 426-432 MHz, 438-444, MHz, and 451-457 MHz and 2360-2400 MHz bands," in "Code of Federal Regulations, Title 47—Telecommunication, Chapter 1—FCC, Subchapter D—Safety and Special Radio Services, Part 95—Personal Radio Services, Subpart I—Medical Device Radiocommunications Service," Tech. Rep. 95.628, 2012.

[21] Federal Communications Commission, "§ 95.627 MedRadio transmitters in the 401-406 MHz band," in "Code of Federal Regulations, Title 47—Telecommunication, Chapter1—FCC, Subchapter D—Safety and Special Radio Services, Part 95—Personal Radio Services, Subpart E—Technical Regulations," Tech. Rep. 95.627, 2012.

[22] Z. S. Inc. (2010). [Online]. Available: www.zarlink.com

[23] J. Bae, N. Cho, and H.-J. Yoo, "A 490 uW fully MICS compatible FSK transceiver for implantable devices," in *Proc. IEEE Symp. VLSI Circuits*, 2009, pp. 36–37.

[24] J. Bohorquez, A. Chandrakasan, and J. Dawson, "A 350 uW CMOS MSK transmitter and 400 uW OOK super-regenerative receiver for medical implant communications," *IEEE J. Solid-State Circuits*, vol. 44, no. 4, pp. 1248–1259, 2009.

[25] J. Pandey and B. Otis, "A sub-100 uW MICS/ISM band transmitter based on injection-locking and frequency multiplication," *IEEE J. Solid-State Circuits*, vol. 46, no. 5, pp. 1049–1058, 2011.

[26] C. A. Balanis, *Advanced Engineering Electromagnetics*, 2nd ed. Hoboken, NJ: Wiley, 2012.

[27] K. S. Yee, "Numerical solution of initial boundary value problems involving Maxwell's equations in isotropic media," *IEEE Trans. Antennas Propagat.*, vol. 14, no. 3, pp. 302–307, 1966.

[28] J. Kim and Y. Rahmat-Samii, "Implanted antennas inside a human body: Simulations, designs, and characterizations," *IEEE Trans. Microwave Theory Tech.*, vol. 52, no. 8, pp. 1934–1943, 2004.

[29] N. Vidal, S. Curto, J. M. Lopez-Villegas, J. Sieiro, and F. M. Ramos, "Detuning study of implantable antennas inside the human body," *Prog. Electromagn. Res.*, vol. 124, pp. 265–283, Jan. 2012.

[30] C. Gabriel, S. Gabriel, and E. Corthout, "The dielectric properties of biological tissues: I. Literature survey," *Phys. Med. Biol.*, vol. 41, no. 11, pp. 2231–2249, 1996.

[31] S. Gabriel, R. W. Lau, and C. Gabriel, "The dielectric properties of biological tissues: II. Measurements in the frequency range 10 Hz to 20 GHz," *Phys. Med. Biol.*, vol. 41, no. 11, pp. 2251–2269, 1996.

[32] S. Gabriel, R. W. Lau, and C. Gabriel, "The dielectric properties of biological tissues: III. Parametric models for the dielectric spectrum of tissues," *Phys. Med. Biol.*, vol. 41, no. 11, pp. 2271–2293, 1996.

[33] K. D. Paulsen, X. Jia, and J. M. Sullivan Jr., "Finite element computations of specific absorption rates in anatomically conforming full-body models for hyperthermia treatment analysis," *IEEE Trans. Biomed. Eng.*, vol. 40, no. 9, pp. 933–945, 1993.

[34] K. S. Kunz and R. J. Luebbers, *Finite Difference Time Domain Method for Electromagnetics*. Boca Raton, FL: CRC Press LLC, 1993.

[35] D. L. Means and K. W. Chan, "Evaluating compliance with FCC guidelines for human exposure to radiofrequency electromagnetic fields," Federal Communications Commission Office of Engineering and Technology, Tech. Rep. 01-01, June 2001.

[36] Federal Communications Commission, "§ 95.1221-RF Exposure," in "Code of Federal Regulations, Title 47—Telecommunication, Chapter 1—FCC, Subchapter D—Safety and Special Radio Services, Part 95—Personal Radio Services, Subpart I—Medical Device RadioCommunication Service," Tech. Rep. 95.1221, 2011.

[37] J. P. Knapp, "ANSYS Inc. request for waiver of 47 C.F.R. sections 1.1307(b) (2) of commission rules; declaratory ruling concerning sections 1.1307(b)(2) of commission rules (DA 11-192)," Federal Communications Commission, Tech. Rep. 11-192, 2011.

[38] P. Soontornpipit, C. M. Furse, and Y. C. Chung, "Design of implantable microstrip antenna for communication with medical implants," *IEEE Trans. Microwave Theory Tech.*, vol. 52, no. 8, pp. 1944–1951, 2004.

[39] A. J. Johansson, "Wave-propagation from medical implants influence of body shape on radiation pattern," in *Proc. 24th Annu. Conf. Annu. Fall Meeting Biomedical Engineering Society EMBS/BMES Conf.*, Houston, TX, 2002, pp. 1409–1410.

[40] E. Y. Chow, B. Beier, O. Yuehui, W. J. Chappell, and P. P. Irazoqui, "High frequency transcutaneous transmission using stents configured as a dipole radiator for cardiovascular implantable devices," in *IEEE MTT-S Int. Microwave Symp. Dig.*, 2009, pp. 1317–1320.

[41] E. Y. Chow, O. Yuehui, B. Beier, W. J. Chappell, and P. P. Irazoqui, "Evaluation of cardiovascular stents as antennas for implantable wireless applications," *IEEE Trans. Microwave Theory Tech.*, vol. 57, no. 10, pp. 2523–2532, 2009.

[42] Cuming Microwave. (2012). [Online]. Available: http://cumingmicrowave.com/

[43] Federal Communications Commission, "§ 95.639 maximum transmitter power," in "Code of Federal Regulations, Title 47—Telecommunication, Chapter 1—FCC, Subchapter D—Safety and Special Radio Services, Part 95—Personal Radio Services, Subpart E—Technical Regulations," Tech. Rep. 95.639, 1999.

[44] Federal Communications Commission, "Investigation of the spectrum requirements for advanced medical technologies, amendment of parts 2 and 95 of the commission's rules to establish the medical device radiocommunication service at 401-402 and 405-206 MHz," Tech. Rep. FCC 10-128, (ET Docket No. 06-135), 2010.

[45] Federal Communications Commission. (2011, Aug. 11). Human torso simulator and testing technique, publication number: 617965. [Online]. Available: https://apps.fcc.gov/oetcf/kdb/forms/FTSSearchResultPage.cfm?switch=P&id=44325

[46] G. Hartsgrove, A. Kraszewski, and A. Surowiec, "Simulated biological materials for electromagnetic radiation absorption studies," *Bioelectromagnetics*, vol. 8, no. 1, pp. 29–36, 1987.

[47] E. Y. Chow, A. Kahn, and P. P. Irazoqui, "High data-rate 6.7 GHz wireless ASIC transmitter for neural prostheses," in *Proc. Engineering in Medicine and Biology Society, 29th Annu. Int. Conf., IEEE*, 2007, pp. 6580–6583.

[48] E. Y. Chow, C.-L. Yang, A. Chlebowski, W. J. Chappell, and P. P. Irazoqui, "Miniature antenna for RF telemetry through ocular tissue," in *Microwave Symp. Dig. IEEE MTT-S Int.*, 2008, pp. 1309–1312.

[49] E. Y. Chow, C.-L. Yang, A. Chlebowski, S. Moon, W. Chappell, and P. Irazoqui, "Implantable wireless telemetry boards for in vivo transocular transmission," *IEEE Trans. Microwave Theory Tech.*, vol. 56, no. 12, pp. 3200–3208, 2008.

[50] E. Y. Chow, C. L. Yang, Y. Ouyang, A. Chlebowski, P. P. Irazoqui, and W. J. Chappell, "Wireless powering and the study of RF propagation through ocular tissue for development of implantable sensors," *IEEE Trans. Antennas Propagat.*, vol. 59, no. 6, pp. 2379–2387, 2011.

[51] E. Chow, B. Beier, W. J. Chappell, and P. P. Irazoqui, "Towards an implantable wireless cardiac monitoring platform integrated with an FDA approved cardiovascular stent," *J. Interventional Cardiol.*, vol. 22, no. 5, pp. 479–487, 2009.

[52] F. C. W. Po, E. de. Foucauld, P. Vincent, F. Hameau, D. Morche, C. Delavaud, R. Dal. Molin, P. Pons, R. Pierquin, and E. Kerhervé, "A fast and accurate automatic matching network designed for ultra low power medical applications," in *IEEE Int. Symp. Circuits Systems*, Taipei, Taiwan, 2009.

[53] R. Elmgvist, J. Landegren, S. O. Pettersson, Å. Senning, and G. William-Olsson, "Artificial pacemaker for treatment of Adams-Stokes syndrome and slow heart rate," *Amer. Heart J.*, vol. 65, no. 6, pp. 731–748, 1963.

[54] W. Greatbatch, "Medical cardiac pacemaker," U.S. Patent 3 057 356, Oct. 9, 1962.

[55] G. D. Nelson, "A brief history of cardiac pacing," *Texas Heart Inst. J.*, vol. 20, no. 1, pp. 12–18, 1993.

[56] (2011). Axis Research Mind. Global cardiac rhythm management (CRM) devices-market growth analysis, 2009-2015. [Online]. Available: www. companiesandmarkets.com

[57] Boston Scientific Corp. [Online]. Available: http://www.bostonscientific.com

[58] R. Bercich, D. Duffy, and P. Irazoqui, "Far field RF powering of implantable devices: Safety considerations," *IEEE Trans. Biomed. Eng.*, to be published.